

## ONLINE APPENDIX

### Supplemental Information to Methods Section

*Participants.* Participants were informed to maintain their typical diet and not to engage in vigorous physical activity for 3 days prior to the study. Two groups were recruited: healthy, non-obese ( $n=20$ ) and obese volunteers ( $n=14$ ) not taking medication known to affect glucose metabolism, and all volunteers had normal renal function. Participants reported less than 90 min of non-vigorous exercise per week and were considered to be sedentary. After giving informed, written consent, each volunteer underwent a medical history, physical examination, screening laboratory tests, a 75 g oral glucose tolerance test and  $\text{VO}_2\text{max}$  test. Mitochondrial respiration data from 3 participants in the lean group were reported previously [1].

*Muscle biopsy and hyperinsulinemic euglycemic clamp.* Participants reported to the Clinical Research Unit at Arizona State University following a 10-h overnight fast. At time  $-60$  min before the start of insulin infusion, a percutaneous biopsy of the *vastus lateralis* muscle was obtained with a Bergstrom cannula under local anesthesia. After a tracer ( $[6,6\text{-}^2\text{H}]$  glucose) equilibration period ( $0.04 \text{ mg kg}^{-1}\text{min}^{-1}$ , 120 min), a primed, continuous infusion of human insulin (Novolin; Novo Nordisk, Princeton, NJ) was started at  $80 \text{ mU/m}^2 \cdot \text{min}$  for 120 min, achieving plasma insulin levels of 1020-1200 pmol/l. Plasma glucose was measured every  $\sim 5$  min throughout the study with a glucose oxidase analyzer (Beckman Instruments, Fullerton, CA) and maintained at euglycemia ( $5 \text{ mmol/l}$ , 90-100 mg/dl) using a variable infusion of 20% dextrose through the antecubital vein catheter. The 20% dextrose solution was enriched with  $[6,6\text{-}^2\text{H}]$  glucose, and the constant infusion of  $[6,6\text{-}^2\text{H}]$  glucose was stopped  $+30$  min into the clamp. Tracer to tracee ratio of glucose ( $[6,6\text{-}^2\text{H}]$  glucose/glucose) was determined via the derivatization product glucose pentaacetate using the Finnigan Trace DSQ GS/MS (Thermo Electron Corporation, Waltham, MA, USA). Selective ion monitoring was used to determine glucose tracer enrichments using fragments ions with  $m/z$  of 200 and 202. Hepatic glucose production and glucose disposal were calculated using steady state equations as detailed here [2].

*Small-scale isolation of mitochondria.* *Vastus lateralis* muscle specimens were trimmed of visible fat and immediately weighed. Two hundred milligrams of muscle specimen (if available, otherwise 100 mg) were minced and subjected to a protease (Type XXIV, Sigma Chemical Co., St-Louis, MO) digestion for 7 min. ellet was resuspended in 100  $\mu\text{l}$  mannitol sucrose buffer (in mM: 220 mannitol, 70 sucrose, 10 Tris-HCl, 1 EGTA) and kept on ice for the duration of the respiration studies. The remainder of the mitochondrial suspension was stored at  $-80^\circ\text{C}$  for proteomic analysis.

*Mitochondrial function assessment-calibration of oxygen electrode.* Oxygen content of the RM was determined with stepwise additions of NADH oxidized by sonicated rat heart mitochondria and using  $\text{Na}_2\text{S}_2\text{O}_4$  to establish chemical zero [6]. The concentrations of NADH standards were spectrophotometrically verified.

*Reactive oxygen species measurement.* We tested the rate of resorufin appearance in the absence of horseradish peroxidase (HRP) in our standard curve of  $\text{H}_2\text{O}_2$  and no

detectable rate of resorufin appearance was measured. We also see no change in fluorescence with incubated rat muscle mitochondria + substrate + oligomycin if HRP is left out of the assay (data not shown), signifying that  $\text{H}_2\text{O}_2$  is the electron acceptor for HRP, and that the assay is indeed measuring the rate of appearance of  $\text{H}_2\text{O}_2$ , which is proportional to reactive oxygen species production (superoxide production =  $2 \times \text{H}_2\text{O}_2$  production in  $\mu\text{mol min}^{-1}\text{mg}^{-1}$ ). The specificity of the Amplex Red assay towards  $\text{H}_2\text{O}_2$  has been addressed by others (see [7] for review), and has been shown to be specific.

*Citrate synthase activity.* Briefly, mitochondria were lysed in 0.1 M Tris containing 0.1 % Triton X-100 (pH 8.1 at 23°C). Mitochondrial lysate (2-10  $\mu\text{g}$ ) was added to 300  $\mu\text{M}$  acetyl coenzyme A and 100  $\mu\text{M}$  5,5'-dithiobis(2-nitro-benzoic acid) in lysis buffer. CS activity was initiated by adding 50  $\mu\text{M}$  final oxaloacetate. CS activity was expressed as  $\mu\text{mol/min g}$  wet muscle weight.

*Calculation of mitochondria recovery.* The mitochondria yield was calculated by taking the ratio of citrate synthase activity isolated (i.e. in the mitochondrial preparation) per mg wet muscle weight to the citrate synthase activity measured in whole muscle per muscle wet weight.

*Mitochondria solubilization.* Mitochondria preparation were homogenized by freeze-thaw ( $3 \times$  liquid  $\text{N}_2$  and 37° C) followed by the addition of an equal volume of 2X lysis buffer (1X, in mM: 50 Hepes, 150 NaCl, 0.02 sodium pyrophosphate, 20 beta-glycerophosphate, 10 NaF, 50 SDS, 0.001  $\text{NaVO}_4$ , 0.001 phenylmethanesulphonylfluoride (PMSF), 10  $\mu\text{g}/\mu\text{l}$  leupeptin and 10  $\mu\text{g}/\mu\text{l}$  aprotinin). The suspension was incubated on ice for 30 min. Protein concentration of the supernatant was determined using Coomassie Plus Protein Assay Reagent (Bio-Rad, Hercules, CA).

*Mass spectrometry.* Samples were desalted using an on-line Nanotrap (Michrom Bioresources). On-line capillary HPLC was performed using a Michrom BioResources Paradigm MS4 micro HPLC (Auburn, CA) with a PicoFrit™ column (New Objective). HPLC separations (300nl/min) were accomplished as follows: linear gradient of 2 to 27% ACN in 0.1 % FA in 70 min, hold 5 min at 27% ACN, hold 5 min at 50% ACN and hold 5 min at 80%. A "top-10" data-dependent tandem mass spectrometry approach was utilized to identify peptides in which a full scan spectrum (survey scan) was acquired followed by collision-induced dissociation (CID) mass spectra of the 10 most abundant ions in the survey scan. The survey scan was acquired using the FTICR mass analyzer in order to obtain high resolution, high mass accuracy data.

*Data analysis and bioinformatics.* Tandem mass spectra were extracted from Xcalibur "RAW" files and charge states were assigned using the Extract\_MSN script, a component of Xcalibur 2.0 SR2 (Thermo Fisher; San Jose, CA). Charge states and monoisotopic peak assignments were then verified using DTA-SuperCharge (msquant.sourceforge.net) [8], before all "DTA" files from each gel lane were combined into a single Mascot Generic Format file. The fragment mass spectra were then searched against the IPI\_HUMAN\_v3.33 database (67 764 entries, <http://www.ebi.ac.uk/IPI/>) using Mascot (Matrix Science, London, UK; version 2.2). The false discovery rate was

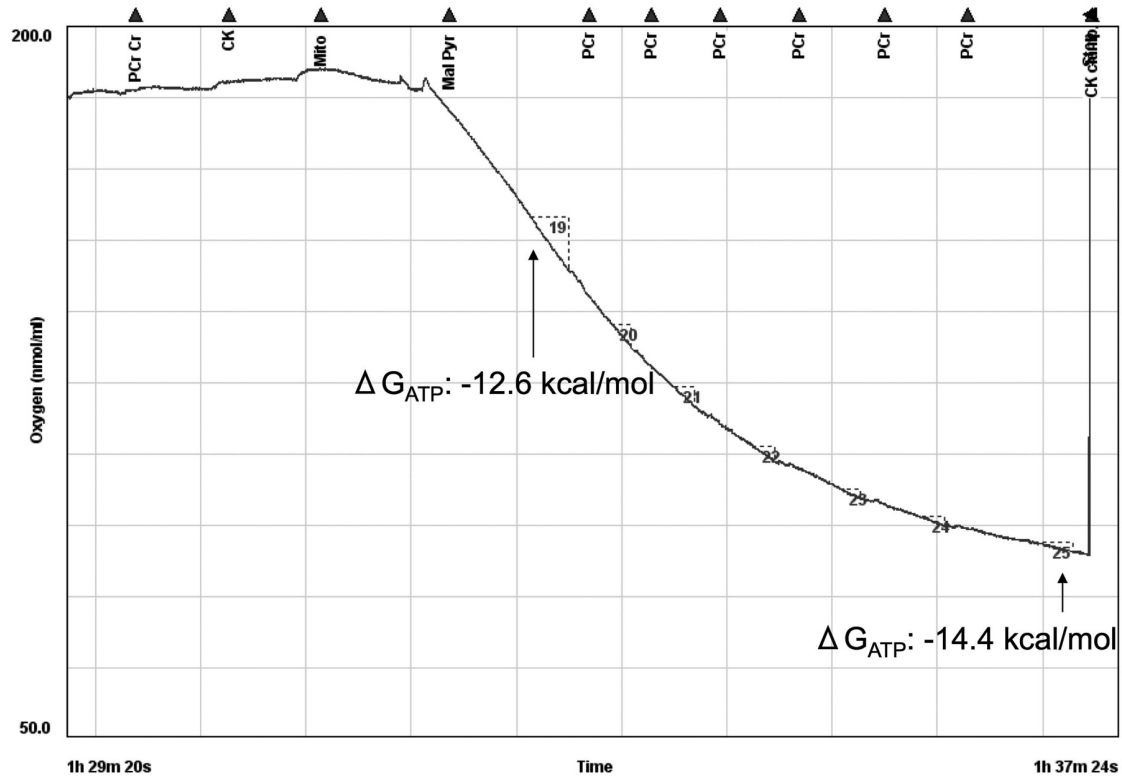
determined by selecting the option to use a "decoy" randomized search strategy that is available in Mascot v2.2 and was found to be < 1% at the protein level. Search parameters used were: 10 ppm mass tolerance for precursor ion masses and 0.5 Da for product ion masses; digestion with trypsin; a maximum of two missed tryptic cleavages; variable modifications of oxidation of methionine and phosphorylation of serine, threonine and tyrosine. Probability assessment of peptide assignments and protein identifications were made through use of Scaffold (version 02\_00\_06, Proteome Software Inc., Portland, OR). Only peptides with  $\geq 95\%$  probability were considered. Criteria for protein identification included detection of at least 2 unique identified peptides and a probability score of  $\geq 95\%$ . Multiple isoforms of a protein were reported only if they were differentiated by at least one unique peptide with  $\geq 95\%$  probability, based on Scaffold analysis. UniProt ([www.pir.uniprot.org](http://www.pir.uniprot.org)) was used to obtain Gene Ontology annotation (GO).

*Immunoblotting.* Mitochondrial lysates (20  $\mu$ g) were resolved on a 4-15% Tris-HCl polyacrylamide gradient gel (Bio-Rad, Hercules, CA). Proteins were transferred to a nitrocellulose membrane and blocked with 5% non-fat milk in 1X Tris-buffered saline (Bio-Rad, Hercules, CA) and 0.2% Tween 20. Membranes were incubated overnight at 4°C in 1% non-fat milk with antibodies specific to human COXIV (Invitrogen, 1:1000) or ALDH6A1 (Abcam, 1:500) and then incubated with a secondary horseradish-conjugated antibody for 1 hr at room temperature (anti-mouse or anti-rabbit IgG, Santa Cruz, CA). Immunoreactive bands were visualized by enhanced chemiluminescence (Western Lightning Plus, Perkin-Elmer, CT).

### **Supplemental Information to Results Section**

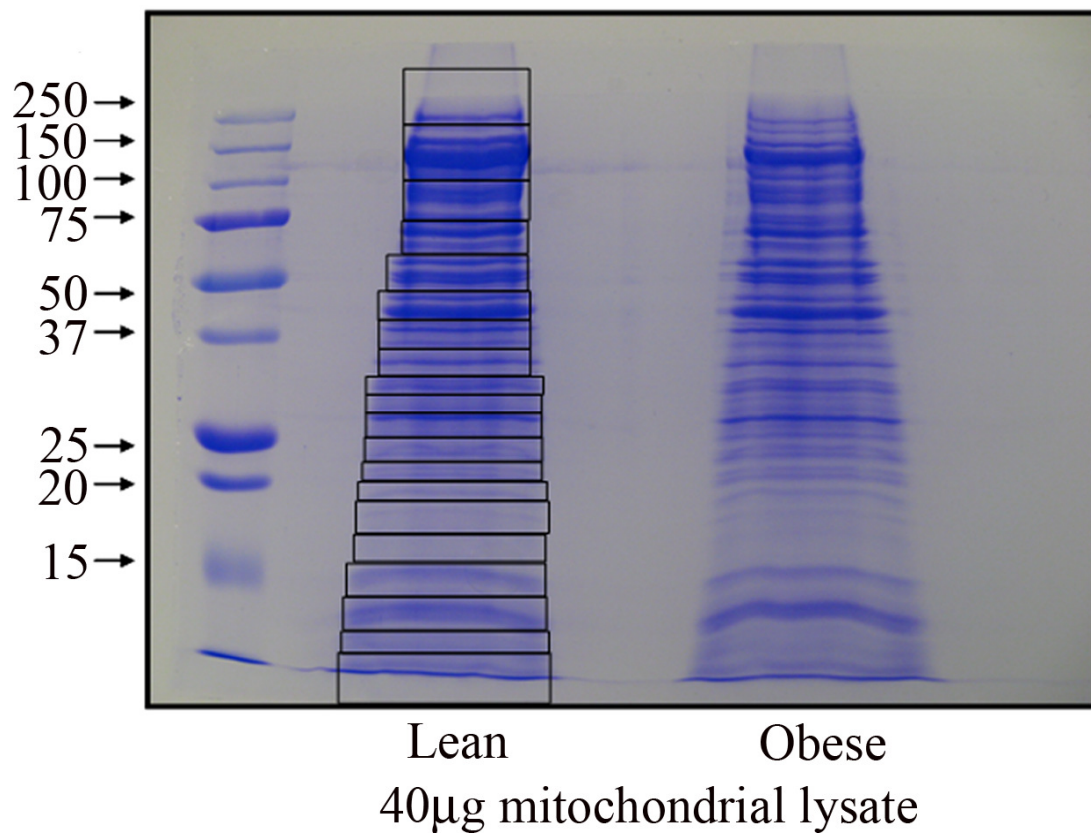
*Differences in mitochondrial protein abundance.* Total spectra assigned to individual proteins were similar between both groups (lean: 35379  $\pm$  425 vs. obese: 35307  $\pm$  422). In line with an identical method published recently [1], on average, 21% of these spectra were generated by myosin isoforms. Approximately 19% of spectra were assigned to proteins not associated to the GO term 5739 (mitochondrion). GO assignment is not perfect; therefore these proteins may be of mitochondrial origin, new uncharacterized mitochondrial proteins or contamination by non-mitochondrial proteins. Contamination by non-mitochondrial proteins is a limitation to using a mitochondria isolation protocol which retains maximal activity of the isolated organelle.

A representative Coomassie-stained gel is included showing a mitochondrial lysate from a lean and obese individual along with the pattern of slices cut (from top to bottom: 1-20) from the gel and processed for mass spectrometry analysis (same pattern cut from obese lane). (Supplemental Figure 2)



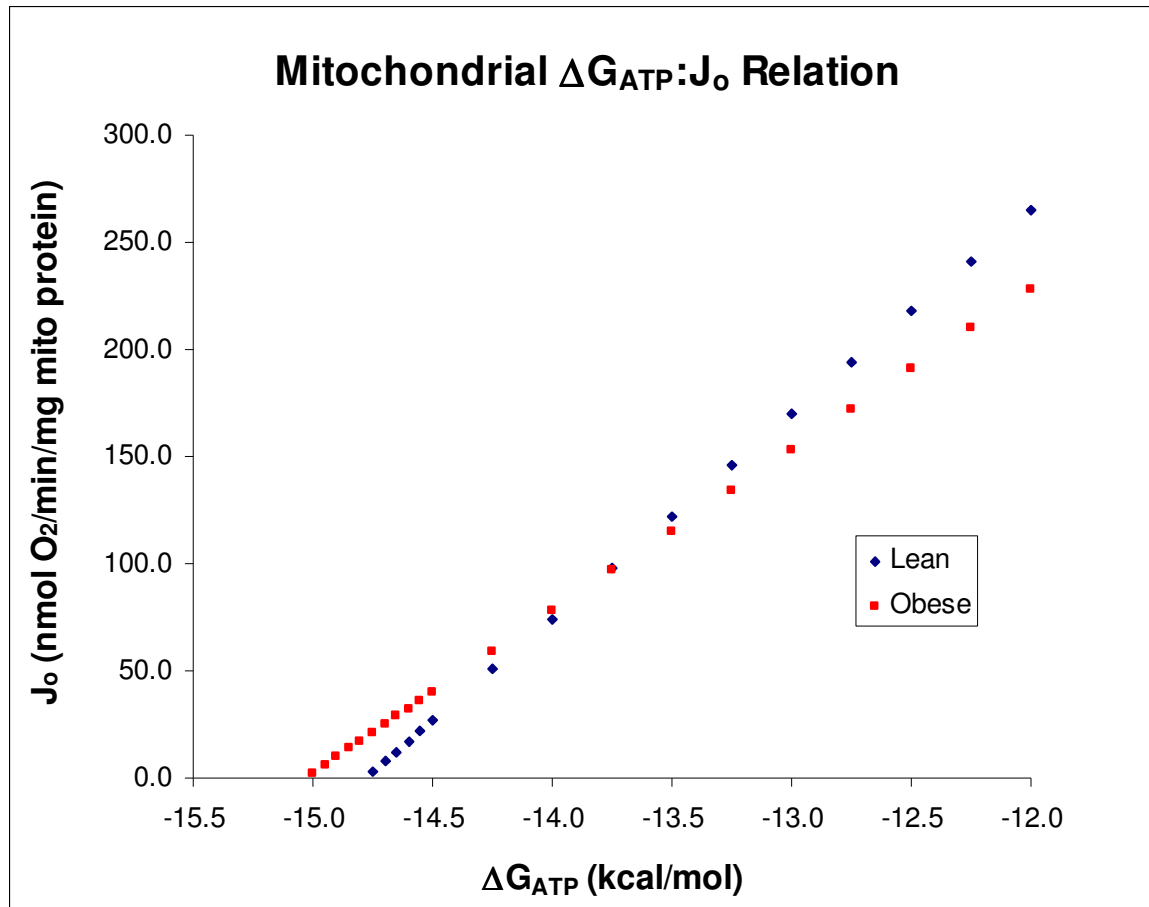
### Supplemental Figure 1.

*Static head*  $\Delta G_{ATP}$ . Isolated mitochondria were challenged with pyruvate + malate at different PCr:Cr ratios. Representative recording by Oxygraph Software displaying the substrate additions over time (in order: Phosphocreatine (PCr), Creatine (Cr), Creatine Kinase (CK), Mitochondria (Mito), Pyruvate (Pyr) and Malate (Mal). Additional boluses of phosphocreatine (PCr) were added to modulate the  $\Delta G_{ATP}$  (i.e. the [ADP], equations described in *Methods*) braking respiration (i.e. lowering of rate of  $O_2$  consumption). A range of  $\Delta G_{ATP}$  were applied to the mitochondria (from -12.6 to -14.4 kcal/mol) representing the spectrum of  $\Delta G_{ATP}$  measured in active SM to that measured at rest.



**Supplemental Figure 2.**

*Comparison of protein abundance differences identified by mass spectrometry with immunoblot analysis.* To visualize protein abundance differences identified by mass spectrometry, immunoblot analyses were performed using two selected proteins for which antibodies were commercially available and which yielded repeatable immunoblots showing a protein band at the correct molecular weight.



### Supplemental Figure 3. $\Delta G_{ATP}$ vs $J_o$ .

Using the creatine kinase clamp (see Methods and Supplemental Figure 1 and Figure 3A), the relationship between mitochondrial O<sub>2</sub> consumption rate ( $J_o$ ) and the extramitochondrial free energy of ATP hydrolysis ( $\Delta G_{ATP}$ ), the “force-flow” relation, was investigated. This “force-flow” relation is a measure of mitochondrial sensitivity to a respiratory control signal. The greater slope exhibited by mitochondria from lean muscle indicates higher control sensitivity i.e., a smaller change in ATP free energy is required to elicit a given change in  $J_o$ . Extrapolation of the relation to the abscissa yields the theoretical ATP free energy that would occur at zero oxidative flux (“static head energy”). In this case, muscle mitochondria isolated from obese individuals exhibit the higher (more negative) value (See Figure 3B). Because the generation of  $\Delta G_{ATP}$  depends on upstream mitochondrial driving forces (protonmotive force and matrix redox potential), higher static head  $\Delta G_{ATP}$  is consistent with resting energetic conditions favoring mitochondrial ROS production.

## Supplemental References

1. Lefort N, Yi Z, Bowen B, Glancy B, De Filippis EA, Mapes R, Hwang H, Flynn CR, Willis WT, Civitarese A, Hojlund K, Mandarino LJ. Proteome profile of functional mitochondria from human skeletal muscle using one-dimensional gel electrophoresis and HPLC-ESI-MS/MS. *J Proteomics* 2009;72:1046-1060.
2. Debodo RC, Steele R, Altszuler N, Dunn A, Bishop JS. On the Hormonal Regulation of Carbohydrate Metabolism; Studies with C14 Glucose. *Recent Prog Horm Res* 1963;19:445-488.
3. Jackman MR, Willis WT. Characteristics of mitochondria isolated from type I and type IIb skeletal muscle. *Am. J. Physiol.* 1996;270:C673-678.
4. Makinen MW, Lee CP. Biochemical studies of skeletal muscle mitochondria. I. Microanalysis of cytochrome content, oxidative and phosphorylative activities of mammalian skeletal muscle mitochondria. *Arch. Biochem. Biophys.* 1968;126:75-82.
5. Jackman MR, Ravussin E, Rowe MJ, Pratley R, Milner MR, Willis WT. Effect of a polymorphism in the ND1 mitochondrial gene on human skeletal muscle mitochondrial function. *Obesity (Silver Spring)* 2008;16:363-368.
6. Estabrook RW, Ronald WEaMEP. *Methods in Enzymology*, Academic Press 1967, pp. 41-47.
7. Tahara EB, Navarete FD, Kowaltowski AJ. Tissue-, substrate-, and site-specific characteristics of mitochondrial reactive oxygen species generation. *Free Radic Biol Med* 2009;46:1283-1297.
8. Forner F, Foster LJ, Campanaro S, Valle G, Mann M. Quantitative proteomic comparison of rat mitochondria from muscle, heart, and liver. *Mol Cell Proteomics* 2006;5:608-619.